Desalination and Water Treatment
www.deswater.com

26 (2011) 287–296
February

1944-3994/1944-3986
doi: 10/5004/dwt.2011.1949

Experimental validation of theoretical correlation for calculation of mass transfer in simple and hybrid solar stills

Khaoula Hidouri[a], Nejib Hidouri[b,*], Romdhane Ben Slama[a], Slimane Gabsi[a], Ammar Ben Brahim[b]

[a]*Engineers National School of Gabès, Analysis Processes Unit, Gabès University, Omar Ibn El Khattab Street, 6029 Gabès, Tunisia*
[b]*Engineers National School of Gabès, Applied Thermodynamics Unit, Gabès University, Omar Ibn El Khattab Street, 6029 Gabès, Tunisia*
Tel. +216 20 979 205; email: n_hidouri@yahoo.com

Received 9 April 2010; Accepted 28 June 2010

ABSTRACT

The present study is based on the use of three correlation groups which are: the Lewis number, the Dunkle and the 'Kumar and Tiwari' correlations for evaluating mass transfer in two types of solar stills. Theoretical results are compared with those obtained experimentally for a Simple Solar Distiller and a Hybrid Simple Solar Distiller/Heat pump stills. Experimental results and those calculated by Lewis number correlation show good agreements. Theoretical results obtained using Dunkle and 'Kumar and Tiwari' correlations are not satisfactory with the experimental ones.

Keywords: Heat and mass transfer model; Simple solar distiller; Hybrid simple solar distiller; Heat pump

1. Introduction

Desalination of ground brackish water by solar powered systems is a practical and promising technology for producing potable water, in the regions which suffer from water scarcity especially in the remote arid areas [1]. The rapid population growth, along with the expected social and economic development will increase the demand for water in such a way that the future water reserve will not meet such a demand.

In remote and arid areas that reveal low infrastructure and in absence of the connection with the national grid, the abundant solar radiation intensity along the year and the available brackish water resources are two favorable conditions for using the solar powered desalination technology to produce fresh water, even for domestic use. A solar desalination technology might be technically and economically viable to cope with water scarcity, and it is recommended to be used in the remote and isolated communities. Desalination of brackish water was expanded rapidly to support urban and industrial developments in the arid areas, the results were published by some researchers in the field of solar desalination [2,3]. In order to enhance the solar stills productivity, numerous groups around the world have contributed to improve the solar desalination technology, by evaluating the influence of some important operating parameters on the system performance. The effect of climatic conditions, design, operational conditions and geographical location on the water productivity were investigated in [4–7] Abdallah et al. [8] studied the single slope solar still. Two absorbing materials types

*Corresponding author.

were used: coated and uncoated porous media (called metallic wire sponges) and black volcanic rocks. Results showed that the uncoated sponge has the highest water collection during day time, followed by the black rocks and then coated metallic wire sponges. Shatat and Mahkamov [9] described the experimental investigations of the performance of a multi-stage water desalination still connected to a heat pipe evacuated tube solar collector with an aperture area of 1.7 m^2. The multi-stage solar still water desalination system was designed to recover latent heat from evaporation and condensation processes in four stages. The variation in the solar radiation during a typical mid-summer day in the Middle East region was simulated on the test rig using an array of 110 halogen floodlights covering the area of the collector. The results of tests demonstrate that the system produces about 9 kg of fresh water per day and has a solar collector efficiency of about 68%. A computer program was developed for transient simulations of the evaporation and condensation processes inside the multi-stage still. Experimental results obtained and theoretical predictions were found to be in good agreement.

El-Sebaii et al. [10] found that the daily total productivity of the still increases with the rise of a wind speed V up to a typical velocity V_t, beyond which the increase in productivity becomes insignificant. The magnitude of V_t is independent of the water mass in each effect, but it showed some seasonal dependence. On a typical summer day, the daily total productivity of the still was found to be 12.635 kg/m^2/d, which agrees well with the results reported in the literature for triple-effect solar stills.

Optimum design parameters for a shallow water basin that produce an average annual solar still yield of 4.15 kg/m^2/d and 6 kg/m^2/d for single and double-effect solar stills, respectively, are given by Al-Hinai et al. [11]. These parameters are: 23° cover tilt angle, 0.1 m insulation thickness and asphalt coating of the solar still.

Palacio and Fernández-Zayas [12] showed that in solar stills with larger aspect ratios, the dominating heat transfer mechanism is convection which is not as efficient as diffusion. More recent analytical studies done in high inclination solar stills by Porta et al. [13], suggest that tall vertex stills are viable and their geometry can be enhanced to facilitate the development of convection vortices (which will compensate for the loss in heat and mass transfer by diffusion) and to improve the heat transfer. Kwantra [14] studied the importance of the water evaporation area in a solar still. He indicated that an enlarged evaporation area results in a more efficient evaporation-condensation process, inducing the increase of the yield. Rubio-Cerda et al. [15] presented a procedure to estimate the glass cover production in double slop solar stills, as a function of the still temperature and the area fraction as an extension of the model proposed by Dunkle.

In this paper, experimental yield obtained by using single and hybrid solar stills is modelled via the use of three theoretical correlation groups, namely: Dunkle, 'Kumar and Tiwari' and Lewis number. This was done in order to find the most accurate one for productivity prediction.

2. Presentation of the correlations groups

Following Kumar and Tiwari [16], the rate of convective heat transfer is given by its general equation as:

$$Q = h_{cw} \cdot A \cdot \Delta T \tag{1}$$

where h_{cw} is the convective heat transfer coefficient, A is the exchange area and ΔT is the temperature difference between the fluid and the inner surface of the condensing cover. The convective heat transfer coefficient can be regarded as a function that depends on the following parameters:

- Geometry of the surface.
- Flow characteristics of the fluid.
- Physical properties of the fluid at the operating temperature.
- Operating temperature range.

Heat transfer is expressed in dimensionless form by Nusselt number which is given by:

$$Nu = \frac{h_{cw} d}{\lambda} = C\left(Gr \cdot Pr\right)^n \tag{2}$$

Here Nu, Gr and Pr are Nusselt, Grashof and Prandtl numbers, respectively. C and n may be constant or variable dimensionless parameters depending on hypothesis established by the authors as we will see later. Grashof and Prandtl numbers are given by:

$$Gr = \frac{g\,\beta\,\rho^2 d^3}{\mu^2}\,\Delta T \tag{3}$$

$$Pr = \frac{\mu\, C_P}{\lambda} \tag{4}$$

The proposed correlations can be presented as follows.

2.1. Dunkel correlation

Dunkle [17] used Eq. (2) for a mean water temperature of the order of 50 °C and Grashof number such that $Gr > 3.2 \cdot 10^5$. Parameters C and n are constant and set to be

0.075 and 1/3, respectively. For this value of exponent n, the heat transfer coefficient becomes independent of the spacing d. The proposed Dunkle's relationship that gives the mass flow rate of condensate can be written as follows:

$$m_{the} = 16.273 \cdot 10^3 h_{cw} \left(\frac{P_w - P_g}{L} \right) \tag{5}$$

The convective heat transfer coefficient is given by:

$$h_{cw} = 0.884 \left[\left(T_w - T_g \right) + \left(\frac{\left(P_w - P_g \right) \left(273 + T_w \right)}{268.9 \cdot 10^3 - P_w} \right) \right]^{\frac{1}{3}} \tag{6}$$

Eqs. (5) and (6) are defined as Dunkle correlation. This correlation is widely used for comparison purposes (Tiwari and Tiwari [18]).

2.2. Kumar and Tiwari correlation

Kumar and Tiwari [16] developed a thermal model to determine the convective mass transfer for different Grashof numbers for solar distillation in passive and active distillation systems for only summer climatic conditions. In their experiments, water temperature exceeds 50 °C and can reach 85.5 °C. Values of C and n are not constant and the methodology used by Kumar and Tiwari [16] for evaluating C and n can be presented as follows:

- mass flow rate of condensate:

$$m_{the} = 0.0163 \left(P_w - P_g \right) \left(\frac{\lambda}{d} \right) \left(\frac{3600}{L} \right) C \left(Ra \right)^n \tag{7}$$

- convective heat transfer coefficient:

$$h_{cw} = \left(\frac{\lambda}{d} \right) C \left(Gr \cdot Pr \right)^n \tag{8}$$

Eqs. (7) and (8) are defined as 'Kumar and Tiwari' model, the Rayleigh number is given by: $Ra = \left(Gr \cdot Pr \right)$, then Eq. (7) can be rewritten as:

$$m_{the} = K \cdot C \cdot \left(Ra \right)^n \tag{9}$$

where

$$K = 0.0163 \left(P_w - P_g \right) \left(\frac{\lambda}{d} \right) \left(\frac{3600}{L} \right) \tag{10}$$

Table 1
Values of C, n and h_{cw} obtained for different inclinations of condensing cover

Obtained values	15°	30°	45°
C	1.418	2.536	0.968
n	0.148	0.158	0.209
Average h_{cw} (W/m²·K)	13.36	16.93	12.84

Taking logarithm on both sides of Eq. (9) gives:

$$\ln \left(\frac{m_{the}}{k} \right) = Ln\, C + n \ln \left(Gr \cdot Pr \right) \tag{11}$$

This linear eq is used to determine values of C and n.

Values of C and n, proposed and tested, take into account the following conditions:

- Effect of solar cavity,
- Operating temperature ranges,
- Orientations of the condensing covers.

Table 1 shows values of C and n as well as the convective heat transfer coefficient used by this model for different inclinations of the condensing cover for a single slope solar still for New Delhi summer climatic conditions. As it can be seen from this table, there are significant changes in the values of C and n with the inclination of the condensing cover. This indicates that C and n are strongly depend on operating conditions.

2.3. Lewis number correlation

Zheng et al. [19] used an electrical resistance immersed in the water in order to increase the water temperature of the basin. In this case, the water temperature exceeds 85.5 °C for a single solar still. On another hand, Chen et al. [20] proposed a relation that includes the characteristic length between the evaporation and the condensation surfaces of the distiller solar still. The convective heat transfer is given by an empirical relation such that:

$$Nu = 0.2 \cdot Ra^{0.26} \tag{12}$$

where $3.5 \times 10^3 < Ra < 10^6$. The convective heat transfer coefficient is given by:

$$h_{cw} = 0.2 \times \frac{l}{d} \times Ra^{0.26} \tag{13}$$

It can be seen in Eq. (13), that the exponential term of the Rayleigh number is not 1/3, and the convective heat

transfer coefficient includes the mean vertical height d between condensation and evaporation surfaces of the solar still, which is an important parameter for analyzing solar stills of various shapes. By considering the existence of great deal of water vapor, the Rayleigh number should be modified, according to the report of Malik et al. [21]. The modified Rayleigh number Ra' is given by:

$$Ra' = \frac{rgbd^3}{ma} DT' \tag{14}$$

The temperature difference is given by:

$$\Delta T' = \left(T_w - T_g\right) + \left(\frac{\left(P_w - P_g\right)\left(273 + T_w\right)}{268.9 \cdot 10^3 - P_w}\right) \tag{15}$$

The Chilton-Colburn [22] analogy can be written as:

$$\frac{Nu}{Pr^n} = \frac{Sh}{Sc^n} \tag{16}$$

Nusselt and Sherwood numbers that express heat and mass transfer, respectively, are given by:

$$Nu = \frac{h_{cw}d}{\lambda}, Sh = \frac{h_m d}{D} \tag{17}$$

Substituting the definition eqs for Nusselt and Sherwood numbers into Eq. (16), we obtain:

$$\frac{h_{cw}\left(d/\lambda\right)}{Pr^n} = \frac{h_m\left(d/D\right)}{Sc^n} \tag{18}$$

Transposing terms, this equation changes into:

$$\frac{h_{cw}}{h_m} = \left(\frac{\lambda}{D}\right)\left(\frac{Pr}{Sc}\right)^n \tag{19}$$

The Lewis number is given by $Le = \frac{Sc}{Pr} = \frac{\alpha}{D}$ and the thermal diffusivity is given by: $\alpha = \lambda / \left(\rho C_P\right)$, then Eq. (19) can be written as:

$$\frac{h_{cw}}{h_m} = \left(\frac{\lambda}{D}\right)\frac{1}{Le^n} = \left(\frac{\alpha \rho C_P}{D}\right)\frac{1}{Le^n} = \rho C_P Le^{1-n} \tag{20}$$

The evaporation rate per unit area of evaporation surface in the still is given by:

$$m_{the} = h_m \left(\rho_w - \rho_g\right) = \frac{h_{cw}}{\rho C_P\, Le^{1-n}}\left(\rho_w - \rho_g\right) \tag{21}$$

ρ_w and ρ_g can be calculated by the perfect gas equation given by:

$$\rho = \frac{M}{R}\left(\frac{P}{T}\right) \tag{22}$$

The evaporation rate equation Eq. (21) becomes:

$$m_{the} = \frac{h_{cw}}{\rho C_P\, Le^{1-n}}\left(\frac{M}{R}\right)\left(\frac{P_w}{T_w} - \frac{P_g}{T_g}\right) \tag{23}$$

Eq. (23) defines the Lewis number correlation, the exponent n is equal to 0.26 [19].

As an important conclusion, all the above correlations differ by their conditions of use such as: the considered water temperature, the values of C and n, the inclination of the glass cover, the characteristic length between water and glass cover and other operating conditions.

The calculations of physical properties of humid air such as: isobaric specific heat C_p, thermal conductivity λ, mass density ρ, dynamic viscosity μ, vapor partial pressures P_w and P_g are based on the correlations given by Jain and Tiwari [23]. Equations for calculation of the above properties are presented in Appendix A.

3. Experimental set up

3.1. Simple solar distiller model

Basin bottom is fabricated from fiber forced plastic material and the absorbed energy is largely transferred to the saline water by conduction and convection modes. A small fraction of the absorbed heat may be lost by conduction into the ground. At the water surface, energy is transferred to the cover by three mechanisms: vaporization, convection and radiation. The vapor is transferred to the cover by free convection of the air in the distiller. Fig. 1 shows the schematic diagram of the simple solar still used and its photograph, area of the basin is equal to 0.4 m^2 (650 mm × 615 mm). The water depth is an operating parameter, in the present study it was kept constant and equal to 30 cm.

3.2. Hybrid simple solar distiller/heat pump model

Vapour-compression cycles can be used as a cooling system, heat pumps or for power production (Organic Rankine Cycle). Although conventional vapor compression refrigeration systems are being widely studied

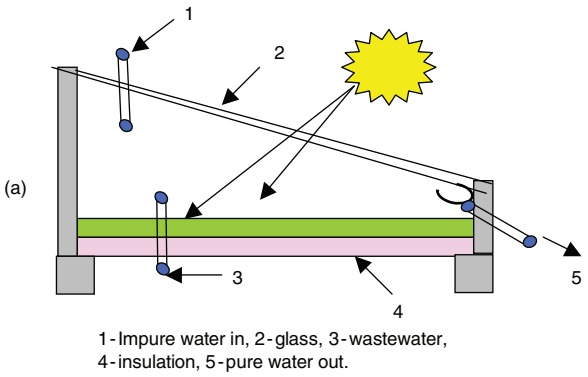

Fig. 1. Simple solar distiller still: a) Schematic diagram of the still, b) Photograph of the SSD still.

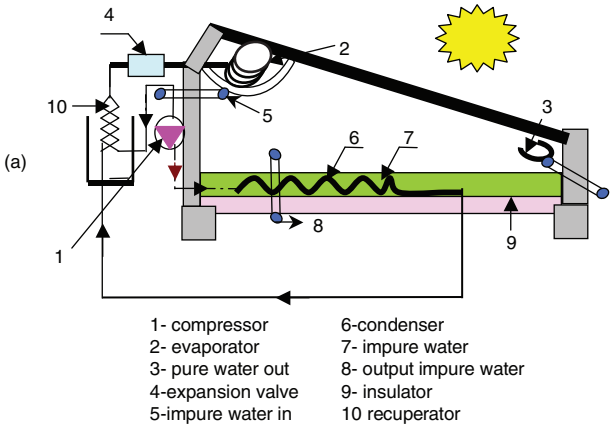

Fig. 2. Hybrid simple solar distiller/heat pump still: a) Schematic diagram of the still, b) Photograph of the SSDHP still.

and used during the last 100 y with machines ranging from small domestic unit of 0.5 ton capacity to air-conditioning plant of 300 ton capacity, solar energy operated vapor compression cooling machines are relatively recent techniques.

A hybrid solar still heat pump is used to enhance the water temperature of basin (having the same dimensions of that used in simple still) to increase the evaporation and enhance the condensation of distillate. Fig. 2 show this configuration. This model corresponds to a vapor compression cycle of refrigeration. In fact, a condenser is immersed in the basin water to increase the water temperature so that the evaporated quantity of water will increase. The evaporator which is located near the upper region of the glass cover enhances the condensation of the water vapor, and the refrigerant after leaving the condenser is introduced into a recuperator filled with fresh water in order to maintain the temperature of the refrigerant at the low level. After that, the refrigerant enters the evaporator at the low pressure inducing the condensation of water vapor. As a consequence, a more quantity of condensed water will be recuperated at the distilled water gutter. The consuming power as compressor works for pumping heat is equal to 0.2 KW.

3.3. Experimental parameters

For the installation, the value (0) is given when the Simple solar distiller (SSD) and the Simple solar distiller hybrid with heat pump (SSDHP) stills are oriented towards the south and the value (1) when the stills are periodically oriented towards the sun (azimuth consideration).

For the glass cover, the value (0) is given when a single glass cover is used and the value (1) for a double glass cover. Similarly, the value (0) is given in absence

of the heat pump and the value (1) is given when the heat pump is used. Table 2 illustrates different studied configurations.

3.4. Instrumentation

Temperature is measured at different points of the system. Glass, water and ambient temperatures are measured by thermometers (with accuracy of 0.1 °C), the reading scale ranges between –50 °C to 300 °C. The distiller output is measured by a graduated test-tube. Solar radiation is measured by a pyranometer mounted near the glass.

4. Results and discussions

The aim of this paper is to use three different correlations in order to compare theoretical results with our experimental work in term of hourly yield. As mentioned above, correlations are as follows: Dunkle [17] given by Eq. (5), 'Kumar and Tiwari' [16] given by Eq. (9) and Lewis number given by Eq. (23). Tables 3, 4, 5 and 6 illustrate a comparison between experimental and theoretical hourly yield for the four studied configurations: two for the SSD and two for the SSDHP models.

Table 2
Operating parameters for different studied configurations

Position	Glass cover	Heat pump compression	Configuration
0	0	0	000
0	0	1	001
1	1	0	110
1	1	1	111

As it can be seen in Table 3, which is related to the '000' configuration, maximum evaporated mass flow rate calculated by using the Dunkle correlation does not exceed 67 $g/m^2 h$, whereas it reaches is 116.46 $g/m^2 h$ with the 'Kumar and Tiwari' correlation. These values are low compared to the experimental results. The analysis of the '110' configuration (Table 5) shows that the theoretical mass flow rate calculated using both the 'Kumar and Tiwari' and Dunkle correlations is higher than that obtained experimentally for $m_{ex} < 200$ g/m^2h, this situation is opposite for $m_{ex} > 200$ g/m^2h. Conclusion can be made that the Dunkle and 'Kumar and Tiwari' correlations are not in good agreement with experimental results obtained from the simple solar still. As it can be seen in Tables 3 and 5, the theoretical yield calculated using the Lewis number correlation is in good agreement with that obtained experimentally.

Tables 4 and 6 show results obtained for the hybrid solar still. In this case, the theoretical mass flow rate calculated by using both the Dunkle and 'Kumar and Tiwari' correlations is generally lower than that obtained experimentally, except the value obtained by the 'Kumar and Tiwari' correlation for $m_{ex} \leq 350$ $g/m^2 h$ for the '001' configuration. As in the simple solar still case, the theoretical mass flow rate calculated by the Lewis number model for the hybrid solar still is in a good agreement with the experimental findings. Thus, for the hybrid solar still, results obtained by the 'Kumar and Tiwari' and Dunkle correlations are not accurate and do not agree with the experimental results.

It is important to notice the considerable increase of the mass flow rate of distilled water in the hybrid solar still compared to the simple still. This is an advantage of the heat pump utilization. In fact, the addition of a condenser causes the increase of the water temperature and consequently enhances the water evaporation process. Further, the use of an evaporator near the glass

Table 3
Experimental and calculated yields: '000' configuration

'000' Configuration			
Experimental yields m_{ex} (g/m^2h)	m_{the} (g/m^2h): Lewis number model	m_{the} (g/m^2h): Dunkel model	m_{the} (g/m^2h): 'Kumar and Tiwari' model
25	29.46	8.29	45.04
30	37.7	10.88	41.10
50	151.7	37.01	91.14
280	250.94	58.03	116.46
277	256.38	67.37	104.12
275	301.43	64.08	112.60
280	256.38	58.03	104.12
200	165	50.8	83.02
100	76.41	49.8	53.71
75	75.05	48.75	20.55

Table 4
Experimental and calculated yields: '001' configuration

'001' configuration			
Experimental yields m_{ex} (g/m²h)	m_{the} (g/m²h): Lewis number model	m_{the} (g/m²h): Dunkel model	m_{the} (g/m²h): 'Kumar and Tiwari' model
270	270.0	50.55	695.58
382	382.4	80.89	678.95
1250	1220.5	125.11	721.38
1450	1220.5	142.27	786.51
1300	1400.0	239.45	786.51
1425	936.9	239.45	770.23
1225	1027.9	173.16	791.85
850	502.6	429.18	631.19
737	429.2	160.76	589.29

Table 5
Experimental and calculated yields: '110' configuration

'110' configuration			
Experimental yields m_{ex} (g/m²h)	m_{the} (g/m²h): Lewis number model	m_{the} (g/m²h): Dunkel model	m_{the} (g/m²h): 'Kumar and Tiwari' model
20	19.12	21.73	22.71
25	13.96	9.55	10.1
25	16.83	10.1	10.22
25	25	49.86	45.92
50	50.02	185.84	170.05
50	50.02	136.98	122.65
200	120.05	301.94	266.71
300	300.22	264.87	234.31
275	131.48	369.72	324.56
250	114.08	363.23	328.95
275	275.96	110	329.9

Table 6
Experimental and calculated yields: '111' configuration

'111' configuration			
Experimental yields m_{ex} (g/m²h)	m_{the} (g/m²h): Lewis number model	m_{the} (g/m²h): Dunkel model	m_{the} (g/m²h): 'Kumar and Tiwari' model
1200	1195.6	843.72	609.3358
1275	1259.96	870.5	521.4131
850	774.94	668.25	492.2529
850	557.8	747.8	435.8
750	508.69	602.71	435.2196
1750	1690	593.08	453.9583
1550	1500	659.11	519.9512
1225	829.46	659.11	519.9512
1025	829.46	746.51	519.9512
950	829.46	907.36	519.9512

cover enhances the increase of the amount of condensed water vapor.

Hidouri et al. [24] also showed that coupling a solar still with a heat pump is a very efficient way to increase the basin water temperature (it reached 82 °C) as well as the temperature difference between basin water and evaporator (it reached 77 °C for the '001' configuration and it did not exceed 28 °C for the '000' one) . This temperature difference ensures the continuity of the distillation process. Further, as the water vapor temperature

Table 7
Square root of mean deviation (e), coefficient of linear correlation (r)

Configuration	'000'	'001'	'110'	'111'
Error (e)	e_{Lewis} = 3.3% e_{Dunkle} = 22% $e_{Kumar\text{-}Tiwari}$ = 5%	e_{Lewis} = 3.7% e_{Dunkle} = 51.4% $e_{Kumar\text{-}Tiwari}$ =43.3%	e_{Lewis} = 8.2% e_{Dunkle} = 16% $e_{Kumar\text{-}Tiwari}$ = 12%	e_{Lewis} = 2% e_{Dunkle} = 54.1% $e_{Kumar\text{-}Tiwari}$ =43.5%
Coefficient of linear correlation (r)	r_{Lewis} = 0.88 r_{Dunkle} = 0.88 $r_{Kumar\text{-}Tiwari}$ = 0.53	r_{Lewis} = 0.86 r_{Dunkle} = 0.45 $r_{Kumar\text{-}Tiwari}$ = 0.85	r_{Lewis} =0.80 r_{Dunkle} = 0.61 $r_{Kumar\text{-}Tiwari}$ =0.83	r_{Lewis} = 0.9 r_{Dunkle} = 0.47 $r_{Kumar\text{-}Tiwari}$ = 0.42

decreases, the experimental yield as well as the convective heat transfer coefficient increase. The use of the double glass cover (i.e., '110' and '111' configurations), results in the increase of the water temperature of the basin. This is due to the fact that, the use of the double glass cover will reduce losses. In such case, the water temperature reached 86 °C. As in the case of the first two configurations, the water vapor temperature considerably decreased when a heat pump was used. It was found that the maximum value of the water vapor temperature was equal to 53 °C and 31 °C, whereas the minimum value is equal to 43 °C and –10 °C for the '110' and '111' configurations, respectively.

A statistical analysis was used to predict the best correlation that fits the experimental results. For this reason, square root of mean percent deviation (e) and coefficient of linear correlation (r) equations were used. They are given by (Chapra and Canale [25]):

$$e = \sqrt{\frac{\sum_{i=1}^{N} (e_i)^2}{N}} \tag{24}$$

where

$$e_i = \left[\frac{x_i - y_i}{x_i}\right] \times 100 \tag{25}$$

Here x_i, y_i and N denote the experimental parameter, its corresponding theoretical value calculated by one of the above correlations and the number of experiments, respectively.

The most familiar measure of dependence between two quantities is the correlation coefficient (r). It is obtained by dividing the standard deviation of the two variables by the product of their standard deviations:

$$r = \frac{\sigma_{xy}}{\sigma_x \sigma_y} \tag{26}$$

If r is equal to zero, there is no need for correlation, when the value of the coefficient r is far from zero, correlations are then used. The standard deviations of x and y are given respectively as follows:

$$\sigma_x = \sqrt{\frac{1}{N}\sum_{i=1}^{N} (x_i = \bar{x})^2} \tag{27}$$

$$\sigma_y = \sqrt{\frac{1}{N}\sum_{i=1}^{N} (y_i - \bar{y})^2} \tag{28}$$

$$\sigma_{xy} = \frac{1}{N}\sum_{i=1}^{N} (x_i - \bar{x})(y_i - \bar{y}) \tag{29}$$

$\bar{x} = \frac{1}{N}\sum_{i=1}^{N} x_i$ is the average value of x and $\bar{y} = \frac{1}{N}\sum_{i=1}^{N} y_i$ is the average value of y.

Since the error (e) denotes the difference between experimental and theoretical values, Table 7 shows that $e_{Lewis} < e_{Kumr\text{-}Tiwari} < e_{Dunkle}$, this means that the Lewis number correlation is the best theoretical correlation compared to the two other correlations. When the coefficient of linear correlation (r) tends towards unity, then the given correlation is the best correlation. Thus, as it can be seen in Table 7, this coefficient ranges between 0.8 and 0.9 for the Lewis number correlation, which is the best found range for both sample and hybrid solar stills compared to the the two other correlations. Generally speaking, the hybrid solar still ('111' configuration) is the best one compared to the other studied configurations.

5. Conclusion

The yield of distilled water obtained by four experimental configurations (in simple and hybrid solar stills) is validated by using three correlation groups (Dunkle, 'Kumar and Tiwari' and Lewis number) for calculation of mass transfer. Results show that the Lewis number correlation is in a good agreement with the experimental mass of distilled water obtained for both simple and hybrid solar stills. The Dunkle model provides more accurate prediction for the simple solar still (in '000'

configuration: e_{Dunkle} = 22%, r_{Dunkle} = 0.88) than for the hybrid solar still (in '111' configuration: e_{Dunkle} = 54.1%, r_{Dunkle} = 0.47). 'Kumar and Tiwari' correlation provides better results for both '001' and '110' configurations compared to the Dunkle correlation. Experimental yields obtained in the hybrid solar distiller/heat pump model (i.e., for '111' configuration) are higher than those obtained with the simple solar still.

Appendix A: Physical characteristics of humid air (Jain and Tiwari [23])

$$L = 2.569 \cdot 10^5 \left(647.3 - T_w\right)^{0.38} \quad \text{(A.1)}$$

$$C_P = 999.2 + 0.1434 \cdot T_w + 1.01 \cdot 10^{-4} \cdot T_w^2 - 6.7581 \cdot 10^{-8} \cdot T_w^3 \quad \text{(A.2)}$$

$$\lambda = 0.0244 + 0.6773 \cdot 10^{-4} \cdot T_w \quad \text{(A.3)}$$

$$\rho_w = \frac{353.44}{T_w + 273.15} \quad \text{(A.4)}$$

$$\rho_g = \frac{353.44}{T_g + 273.15} \quad \text{(A.5)}$$

$$\mu = 1.718 \cdot 10^{-5} + 4.620 \cdot 10^{-8} \cdot T_w \quad \text{(A.6)}$$

$$P_w = \exp\left(25.317 - \frac{5144}{273.15 + T_w}\right) \quad \text{(A.7)}$$

$$P_g = \exp\left(25.317 - \frac{5144}{273.15 + T_g}\right) \quad \text{(A.8)}$$

$$\beta = \frac{1}{273.15 + T_i} \quad \text{(A.9)}$$

$(T_i = T_w, T_g)$

Symbols

C — unknown constant in Nusselt number expression
C_p — isobaric specific heat, J/kg·K
D — diffusivity coefficient of water vapor, m²/s
d — mean vertical height between condensation and evaporation surfaces, m
e — square root of mean percent deviation
g — gravity acceleration, m/s²
Gr — Grashof number
h_{ev} — evaporative heat transfer coefficient, W/m²·K
h_{cw} — convective heat transfer coefficient, W/m²·K
h_m — convective mass transfer coefficient, m/s
L — latent heat of vaporization, J/kg
Le — Lewis number
M — molecular weight of water vapor, kg/mol
m_{ex} — experimental mass of condensate, kg/m²·h
m_{the} — theoretical mass of condensate given by type of correlation, kg/m²·h
n — unknown constant in Nusselt number expression
Nu — Nusselt number
Pr — Prandtl number
P_g — partial saturated vapor pressure at glass temperature, N/m²
Pw — partial saturated vapor pressure at water temperature, N/m²
R — universal gas constant, J/mol·K
Ra — Rayleigh number
r — coefficient of linear correlation
Sc — Schmidt number
Sh — Sherwood number
T_a — ambient temperature, °C
T_g — temperature of glass, °C
T_w — temperature of water, °C

Greek letters

α — thermal diffusivity of humid air, m²/s
β — thermal expansion coefficient, K⁻¹
λ — thermal conductivity of humid air, W/m·K
μ — dynamic viscosity of humid air, Pas
ρ_g — density of vapor at glass surface, kg/m³
ρ_w — density of vapor at water surface, kg/m³
σ_{xy} — standard deviation of xy

References

[1] G.R. Lashkaripour and M. Zivadar, Desalination of brackish water in Zahedan city in Iran, Desalination, 177 (2005) 1–5.
[2] B. Bouchekima, A small solar desalination plant for the production of drinkable water in remote arid areas of southern Algeria, Desalination, 159 (2003) 197–204.
[3] J. Joseph, R. Saravanan and S. Renganarayanan, Studies on a single-stage solar desalination system for domestic applications, Desalination, 173 (2005) 77–82.
[4] H.AL-Hinai, M.S. AL-Nassiri and B.A. Jubran, Parametric investigation of a double effect solar still in comparison with a single-effect solar still, Desalination, 150 (2002) 75–83.
[5] B.L. Akash, M.S. Mohsen and W. Nayfeh, Experimental study of the basin type solar still under local climate conditions, Energ. Convers. Mange., 41 (2000) 883–890.
[6] J.A. Duffie and W.A. Beckman, Solar Engineering of Thermal Processes, John Willey and sons Inc. (1980).
[7] M. Boukar and A. Harmim, Parametric Study of a vertical solar still under desert climatic conditions, Desalination, 168 (2004) 21–28.
[8] S. Abdallah, M.M. Abu-Khader and O. Badran, Effect of various absorbing materials on the thermal performance of solar stills, Desalination, 242 (2009) 128–137.
[9] M. Shatat and K. Mahkamov, "Determination of rational design parameters of a multi-stage solar water desalination still using transient mathematical modelling" Rene. Energ., 35 (2010) 52–61.
[10] A.A. El-Sebaii, Thermal performance of a triple solar still, Desalination, 174 (2005) 123–137.

[11] H. Al-Hinai , M.S. Al-Nassri , B.A. Jubran, Parametric investigation of a double-effect solar still in comparison with a single-effect solar still, Desalination, 150 (2002) 75–83.
[12] A. Palacio, J.L. Fernández-Zayas, Numerical analysis of greenhouse-type solar stills with high inclination, Sol. Energy., 50 (1993) 469–476.
[13] M.A. Porta, J.L. Fernández-Zayas, N. Chargoy, Influencia de la distancia vidro-agua destiladores solares de caseta, ANES (1994).
[14] H. Kwantra, Performance of a Solar Still: Predicted effect of enhanced evaporation area on yield and evaporation temperature, Sol. Energy., 56 (1996) 261–266.
[15] E. Rubio-Cerda, M.A. Porta-Gándara, J.L. Fernández-Zayas, Thermal Performance of the condensing covers in a triangular Solar Still, Renew. Energ., 27 (2002) 301–308.
[16] S. Kumar, G.N. Tiwari, Estimation of convective mass transfer in solar distillation systems, Sol. Energy., 57 (1996) 459–464.
[17] R.V. Dunkle, Solar water distillation. The roof type still a multiple effect diffusion still, International Development in Heat Transfer, ASME (1961) 895–902.
[18] G.N. Tiwari, A.K. Tiwari, Solar Distillation Practice for Water Desalination Systems, Anamaya Publishers, New Delhi (2008).
[19] H. Zheng, X. Zhang, J. Zhang, Y. Wu, A group of improved heat and mass transfer correlations in solar stills, Energ. Convers. Mange., 43 (2002) 2469–2478.
[20] Z. Chen, X. Ge, X. Sun, L. Bar, Y.X. Miao, Natural convection heat transfer across air layers at various angles of inclination, Engineering Themophysics: (Special Issue for US-CHINA, Bination Heat Transfer Workshop) (1984) 211–220.
[21] M.A.S. Malik, G.N. Tiwari, S. Kumar, M.S. Sodha, Solar distillation, Oxford, Pergamon Press, UK (1982).
[22] T.H. Chilton, A.P. Colburn, Mass transfer (absorption) coefficients, Industrial and Engineering Chemistry, 26 (1934) 1183–1187.
[23] D. Jain, G.N. Tiwari, Thermal aspect of open sun drying of various crops, Energy., 28 (2003) 37–54.
[24] K. Hidouri, A. Ben Hmiden, R. Ben Slama, S. Gabsi, Effects, of SSD and SSDHP on convective heat transfer coefficient and yields, Desalination, 249 (2009) 1259–1264.
[25] S.C. Chapra, R.P. Canale, Numerical Methods for Engineers, Mc Graw-Hill, New York (1989).